Using an off-the-shelf rigid gripper to grasp objects of different strengths and compliances

Kate Sullivan

A thesis
submitted in partial fulfillment of the
requirements for the degree of
Master of Science in Electrical Engineering

University of Washington

2023

Reading Committee:

Howard Chizeck, Chair

Aaron Marburg

Kim Ingraham

Program Authorized to Offer Degree:

Electrical Engineering

University of Washington

Abstract

Using an off-the-shelf rigid gripper to grasp objects of different strengths and compliances

Kate Sullivan

Chair of the Supervisory Committee:
Professor Howard Chizeck
Department of Electrical and Computer Engineering

Robotic grippers are being increasingly used in everyday tasks and complex missions that require the ability to perform a range of grasps. Rigid grippers have been used for decades since their start in industrial applications, but their inability to grasp delicate objects has led to the development of soft grippers. While soft grippers are showing promising results in many applications, they often are limited by low grasp forces and availability. This paper presents an algorithm for using an off-the-shelf rigid gripper to grasp objects of different strengths and compliances, without the need for tactile sensors or modifications. The algorithm was used to successfully grasp a variety of objects, most notably a potato chip and a highly compliant paper cup.

1. Introduction

The challenge of grasping delicate and compliant objects is a trending topic in the robotics community [1], [2], [3], [4], [5], [6], [7], [8], [9], [10], [11]. Rigid grippers have been well established as robust, reliable, and widely available end-effectors for applications such as industrial uses, underwater missions, and many others. They are recognized for their ease of use, precision, and ability to apply high grasping forces to objects [1], [5], [7], [9]. As robots are being used in a wider range of applications that require more delicate grasps, however, their limited force control and ability to perform gentle grasps has caused researchers to look for alternative solutions.

In recent years, there has been a significant shift from conventional rigid grippers and actuators to soft-robotics in order to address the issue of grasping delicate and compliant objects. Soft-robotics solutions range from soft actuators to achieve more precise force control and variable stiffness grippers [1], [2], [4], [5], [6], [7], [8], [9]. Many of these new designs have proven successful in providing delicate grasps, but they are often limited by their low grasping forces, complexity, and need for maintenance [1], [5], [11], [12]. There have been efforts to design rigid grippers to have better force sensing and control systems, but these designs can be high-cost and complex [3], [10], [11]. To the knowledge of the author, little research has been done to stretch the grasping possibilities of existing rigid grippers without altering the hardware.

This research began as a part of a larger project that aims to use a semi-autonomous robot in a variety of underwater missions ranging from infrastructure maintenance to biological sampling. The Bravo 7 manipulator from Blueprint Labs was purchased as a part of the larger project and came with a standard rigid gripper. Given the ultimate goal of the project, the gripper will require the ability to apply a range of grasps to a variety of objects. Because of the acknowledged limitations of rigid grippers, the goal of this research is to develop an algorithm to use this available, off-the-shelf rigid gripper to automatically grasp objects of different compliances and strengths without the need for additional tactile sensors. This document details the methods used to achieve such a goal beginning with an overview of the available hardware and software in Section 2. The development of a preliminary grasping algorithm is described in Section 3 along with test results. With insight gained from experiments done in Section 3, two sub-algorithms for detecting and characterizing objects are discussed in Section 4 and Section 5. And finally, Section 6 provides the results from the adjusted algorithm which first detects when contact is made with an object and then applies an informed grasp based on the object's properties.

2. Hardware/Software

For this research, the Bravo 7 Arm from Reach Robotics was used with their standard interlocking quad jaws gripper shown in Figure 1. Reach Robotics' communication protocol was used to control the gripper via ethernet, with the ability to send position, relative position, velocity, and electrical current commands to the gripper's actuator. This section details the gripper specifications and control modes.

Figure 1. Reach Robotics Bravo 7 manipulator (left) and their standard interlocking quad jaws gripper (right).

2.1. Gripper specs

The gripper in this model is actuated using a linear pushrod with a range of motion of roughly 33mm. When the pushrod is fully extended (wide open), the jaws have a tip to tip distance of 130 mm and a maximum width of 145 mm. According to Reach Robotics, the grabber close force can reach up to 1000 N. Additional specifications can be found in the datasheet in Appendix A.

2.2. Control Options

The gripper can be controlled using position, velocity, or current commands. In this research, relative position and current commands are used, while the absolute pushrod position, velocity, and current are sampled. The range of operating current for actuating the gripper is -1840 mA for closing and +3400 mA for opening. The update rate for commands and sampling was determined experimentally to be roughly 700 Hz.

Figure 2 shows the available sensor readings with respect to each input. The first row shows the current measurements under current (a), velocity (b), and position (c) inputs. These three graphs are displayed with a range of 300 mA, illustrating that there is significant noise in the signals. The lowest noise in the current signal occurs when current is used as the input. The second row shows velocity measurements under each control input with a range of 1.5 mm/s. There is again significant noise in every signal, but when velocity is used as the input (e), the signal is most stable. The third row shows 25 points of position data under each control input. In all cases, the position changed linearly with time with little some variation between steps.

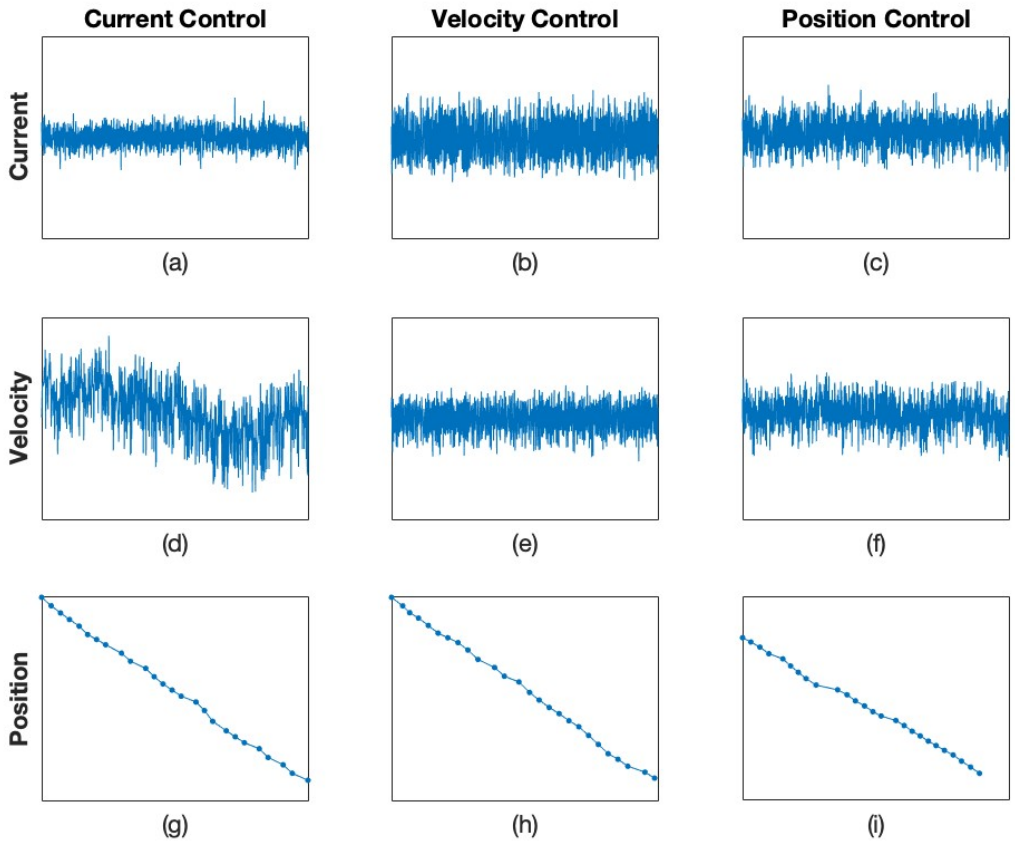

Figure 2. Current, position and velocity readings under each control option. The first column shows the various readings when a current command is used to move the gripper. The second column shows each signal when position commands are used. And the third column shows each signal when velocity commands are used.

3. Grasping objects of different compliances: Part 1

This research began with the goal of using a rigid, off-the-shelf gripper to automatically grasp objects of different strengths and compliances, without the need for additional tactile sensors. Position control is the recommended mode of operation due to its reliability and ease of use. A major issue, however, is the inability to know the force of

the grasp being applied to an object. Because of this limitation, current control was explored as an option to control the amount of force applied to an object. Once the force data was collected and analyzed, an algorithm for automated grasping was developed and tested on various objects both in air and underwater.

3.1. Force data

An ATO Load cell was used to determine the applied force of the gripper at each input current between 0 and 1000 mA using step sizes of 50 mA. The load cell was placed between the fingertips of the jaws, as shown in Figure 3, for repeatability purposes. The gripper was held at each current for 50 samples to ensure steady-state behavior.

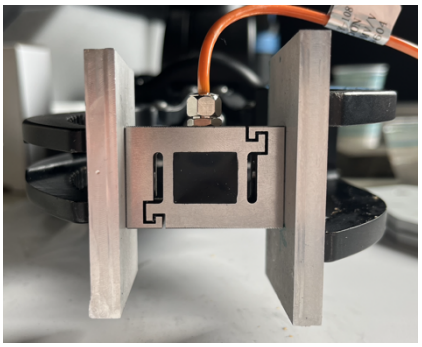

Figure 3. The ATO load cell placed between the fingertips of the end-effector for force data collection. Aluminum plates were secured to each side of the load cell to provide a flat surface for the jaws to contact.

Figure 4 shows the applied force to the load cell with respect to the input current for three runs of this experiment.

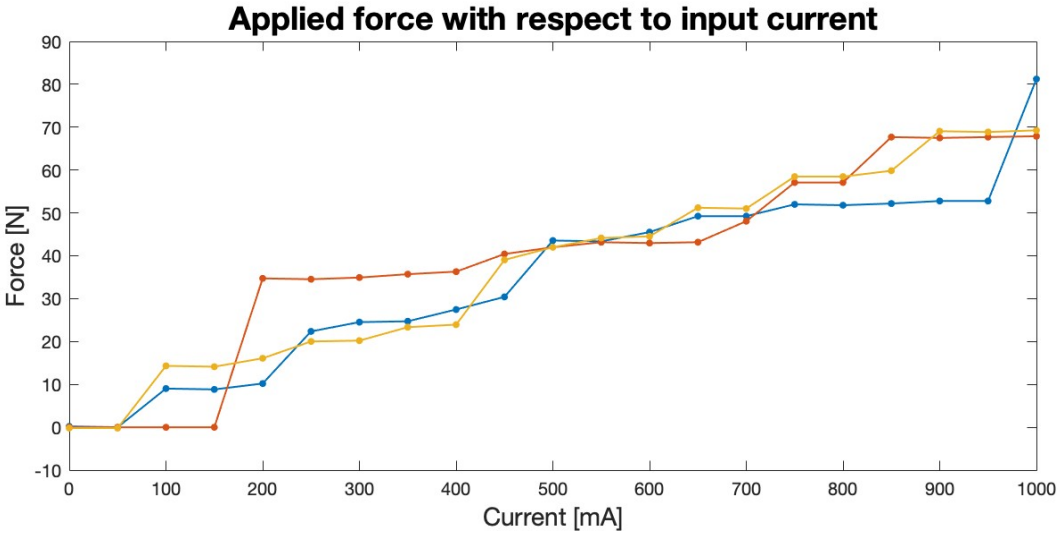

Figure 4. Gripper closing force applied to a load cell at different input current values ranging from 0 to 1000 mA. Each line is a separate trial done for repeatability.

The results in Figure 4 show a fairly linear relationship between the input current used to drive the gripper and the closing force applied by the gripper. Despite this clear trend, there is some variation in the force readings at respective current values. These variations are especially significant at lower current values, which poses an issue when using current to grasp delicate objects.

A second experiment was done similar to the one described previously, but this time with the jaws starting fully open in order to understand the impact that momentum has on the force experienced by an object. The force experienced by the load cell under currents ranging from 150 mA to 400 mA is shown in Figure 5. The values by each peak are the difference in force between the peak force and the steady-state force. This experiment demonstrates the significance of how the impact from the jaws closing on an object can cause a spike in the force experienced at different input currents.

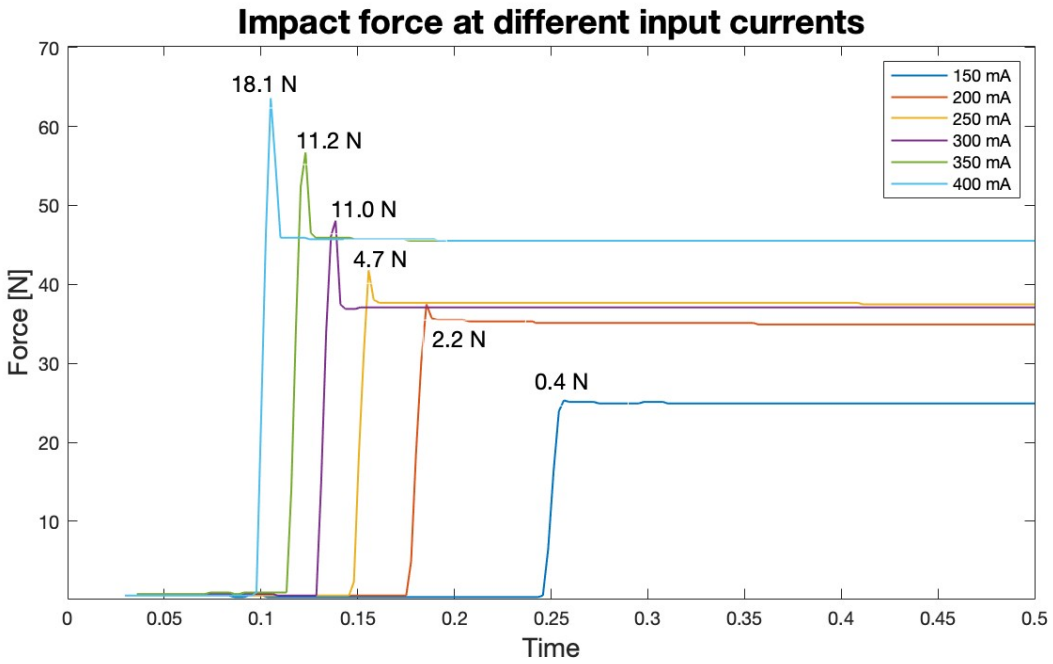

Figure 5. The applied force of the gripper jaws at current values between 150 mA and 400 mA with respect to time. The values at each peak show the difference between the max force and the steady-state force.

These force experiments revealed two major challenges associated with using input current as a means to grasp objects. There is significant variation in applied force at different current values and even at low current values, an object may experience higher forces on impact than desired. Despite these downsides, there were several valuable discoveries made during these experiments:

1. Increasing the input current generally causes an increase in applied force.
2. Though not very precise, a constant current maintains a constant applied force once it has reached steady-state.
3. When the input current is set to 0 mA, the gripper maintains a small applied force of up to 1.8 N due to mechanical properties of the actuator.
4. In order to cause motion, the gripper requires 100 - 200 mA. Setting the current to +50 mA, say, would not cause motion but it would offset some of the frictional forces of the actuator, creating a near net-zero-torque for the gripper.

This information is helpful moving forward and the mechanical resistance of the gripper actuator may be leveraged, especially for delicate objects.

3.2. Position-Current Control Algorithm

Based on the observations made in Section 3.1, there are two main ideas important for a grasping algorithm that would work for delicate objects:

1. The gripper should come in contact with the object slowly to avoid significant impact force.
2. Once contact has been made with an object, a specified current can be used to apply a force within a safe range. For delicate objects, 0 mA or even +50 mA of input current may be appropriate to maintain enough force to hold the object. Recall that the +50 mA offsets some of the frictional forces, creating a looser grip.

To achieve each of these goals, a combination of position and current control can be used where the gripper begins closing using small position changes and then switches to current control once contact is made. Since this process should be automated, however, there is a question of how contact is determined. To address this issue, the algorithm relied on the resistance of the object being grasped as a means of detection. Instead of using position commands to close until contact and then switching to current control, the algorithm instead switches between position and current control in a continuous loop. Figure 6 illustrates how the algorithm is implemented.

```
while True:
    close gripper slightly
    set current to 0 mA
```

Figure 6. Pseudocode showing the algorithm used to automatically grasp an object. The 0 mA highlighted in blue can be changed depending on the object.

This basic loop allows the gripper to continue closing while no object is yet contacted but then allows the object to push back once contact is made. The current value, highlighted in blue in Figure 6, is chosen based on the object. For fragile objects, for example, 0 to +50 mA may be used where as a stronger closing current may be more appropriate for stronger objects with more resistance or elasticity. If the current value is chosen properly, the gripper should compress the object slightly after being given the position command and then be pushed slightly back open when in current control, resulting in a subtle, steady-state oscillation illustrated in Figure 7.

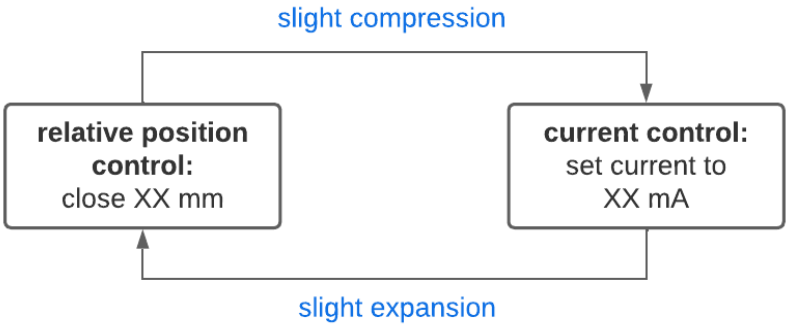

Figure 7. An illustration of how the gripper behaves once contact with an object is made. A position command causes the jaws to close slightly and compress the object. A current command then allows the object to push back against the jaws. This process causes a slight oscillation. The position change at each step and the current input can be adjusted by the user to best suit the object.

3.3. Discussion of results

This algorithm was tested both air and underwater on various objects, shown in Figure 8. Objects such as plastic cups (a and e), a whiteboard eraser (b), a clementine (c), a kiwi (f), and a tomato (g) were grasped with ease and without causing damage. The most challenging object that was successfully grasped was a potato chip, shown in Figure 8d.

(a) (b) (c) (d)

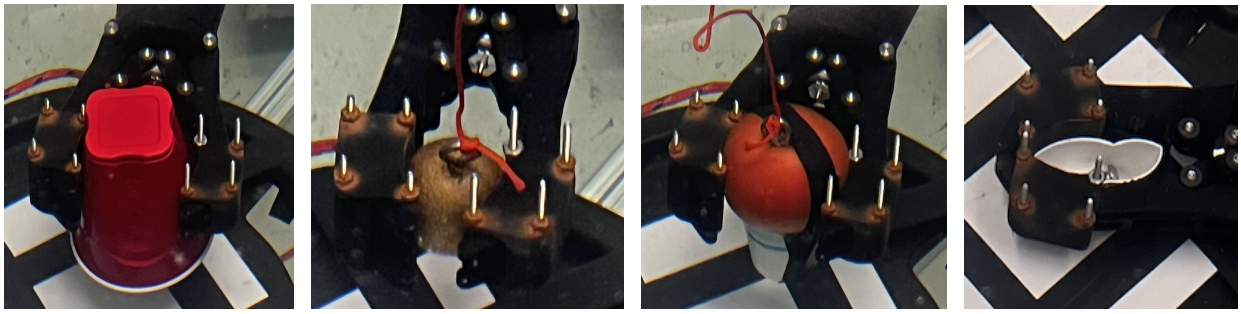

(e) (f) (g) (h)

Figure 8. Grasp tests on various objects in air and underwater. The first row shows for successful grasps in air of a plastic cup (a), a whiteboard eraser (b), a clementine (c), and a potato chip (d). The bottom row shows three successful grasps under water of a plastic cup (e), a kiwi (f), and a tomato (g). The algorithm failed to grasp a paper cup (h) without crushing it.

This algorithm worked for rigid and strong objects, but it failed on highly compliant, delicate objects, such as the paper cup as shown in Figure 8h. While the gripper itself is capable of holding such objects, this case was essentially an issue of detection. In order to perform a successful grasp, this algorithm relies on two ideas: first being that the object has a high enough spring constant to push back on the gripper while current control is being used. In the case of the paper cup, the gripper was never met with enough resistance to create that desired steady-state oscillatory behavior. Additionally, this algorithm is limited to known objects with known properties. If the selected current is not appropriate for the object, there is a chance that the gripper will continue to close and crush the object or that the gripper will not apply enough force to hold the object. These results lead to further research into using the gripper for object detection and characterization. The following sections detail an adjusted algorithm, illustrated in Figure 9, that first detects an object, characterizes the object in terms of strength and rigidity, and finally makes a better informed grasp.

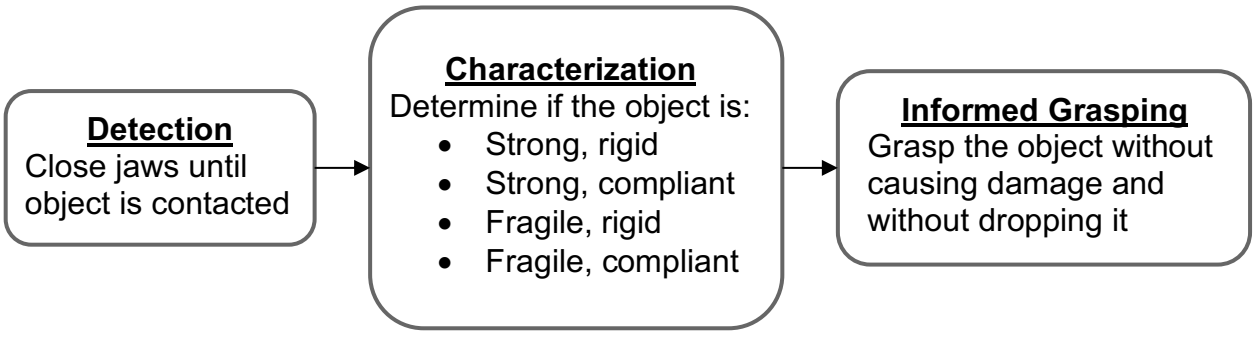

Figure 9. The process needed to automatically grasp objects, including highly compliant objects and those with unknown properties.

4. Detection

As discussed in the previous section, the paper cup is a challenging object because of its high compliance. The previous algorithm relied on an object's elasticity to push back against the gripper to avoid being crushed and therefore it does not perform well on compliant objects. A new method is required to signal when an object is contacted. This section outlines the development of a detection algorithm to address this problem.

4.1. Overview of approach

The results from the initial algorithm showed that a compliant object like the paper cup does not have enough elasticity to push the gripper back open; however, it may still impact the gripper behavior. The new approach for object detection uses a constant input current to close the jaws while monitoring the velocity. If the velocity decelerates beyond a threshold, detected by baseline tests, contact with an object will be assumed and the gripper will stop. To begin, an input current of -150 mA was used to close the gripper. This value was used because it is the lowest current that reliably sets the jaws in motion. This section walks through the development, testing and results of the detection algorithm.

4.2. Baselining

The first step in implementing this algorithm is to collect baseline data of the gripper to determine first, if the velocity of the actuator when no object is present is consistent and second, if there is a noticeable difference in the data when an object is present. To determine the first point, the jaws were set to a fully open position and then closed using an input current of -150 mA. Figure 10 shows the results from several tests. The data follows a clear, repeatable trend but has significant noise and changes with respect to position. Oscillations can be observed at several frequency and are likely due to the current control and hardware properties. How the noise and variation are handled is discussed later in Section 4.3.

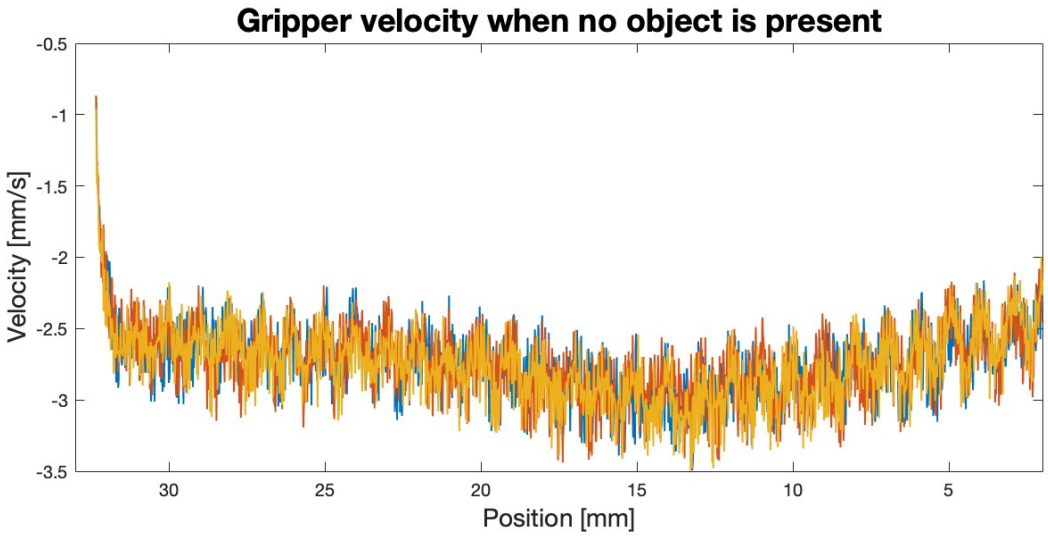

Figure 10. A graph showing the velocity of the gripper with respect to position when no object is present. In addition to noise, a sinusoidal pattern is observed. Multiple data sets are shown to confirm the repeatability of the signal.

Knowing that the velocity of the gripper actuator follows a repeatable trend, the same test was run with a paper cup present to determine if there is a noticeable divergence from the baseline data when no object was present. Figure 11 shows the resulting velocity data from the cup run overlaid with a run with no object present. There is a significant divergence from the baseline velocity when the cup was present. By viewing this data, it is clear that an object is present, but a quantifiable process for determining a detection. This process is outlined in Section 4.3.

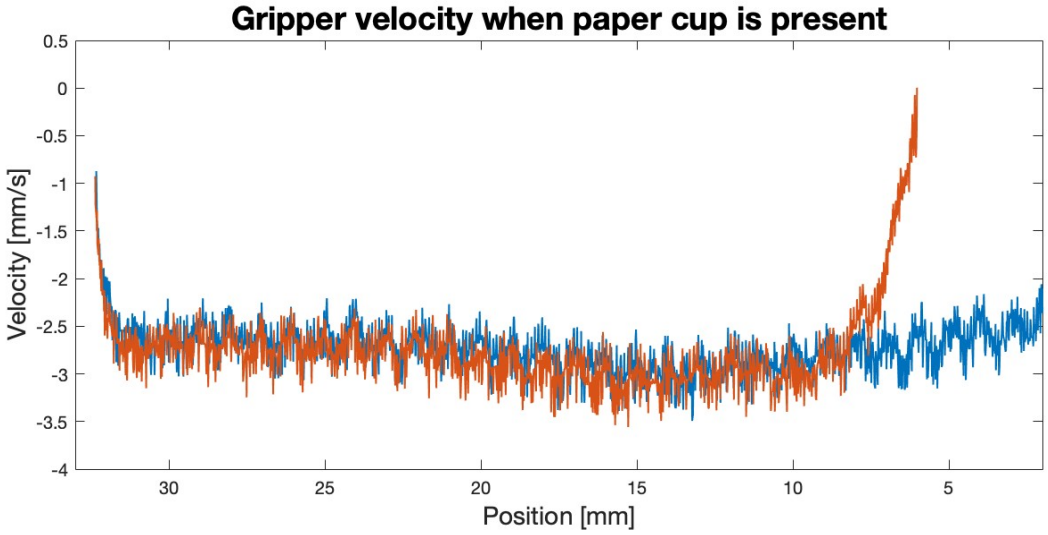

Figure 11. Velocity of the gripper with respect to position when no object is present (blue) and when a compliant paper cup is present (red). There is a clear divergence after the paper cup is contacted.

4.3. Regression and Detection Method

While the velocity readings when no object is present are repeatable, they vary with position and therefore a single value threshold would not be sufficient for detecting objects of different size. A fourth degree polynomial regression was applied to the baseline velocity data to model the expected velocity at each position. This model was then offset to encapsulate the noise readings closer to zero and is used as a threshold for object detection. Both the regression model and the offset are shown in Figure 12.

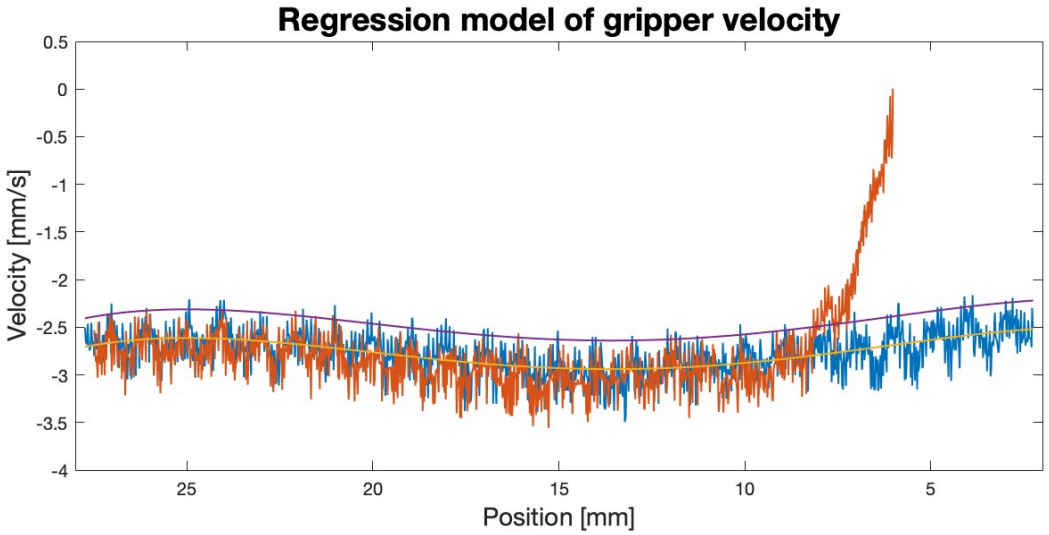

Figure 12. Regression model of expected gripper velocity with respect to position. The blue and red datasets are the same as in Figure 11. A regression line (yellow) based on the blue data models the expected velocity of the gripper at each position. This line was offset (purple) to act as a threshold for detection.

Even with the offset, there are still some data points that fall above the threshold that are not due to contact with an object. To address this, the algorithm requires that a specified number of consecutive data points fall above the threshold in order to be considered a true detection. This process is illustrated in Figure 13.

```
begin closing jaws with current input of -150 mA

count = 0 //consecutive velocity readings over predicted velocity

while no object is detected:

     predicted_velocity = regression_model(position)

     if measured_velocity > predicted_velocity:
          count = count + 1
     else:
          count = 0

     if count > n:
          object is detected, exit while loop

stop the jaws
```

Figure 13. Pseudocode outlining how the regression model is used to determine if an object is present or not. At each sample, the measured velocity is compared to the velocity predicted by the regression model. If a specified number of consecutive data points fall above the predicted values, an object is assumed to be present, and the gripper is stopped.

4.4. Results and Analysis

Despite the data clearly indicating the presence of an object, the paper cup was regularly being crushed when testing this algorithm. Several hypotheses were made as to why these failures were occurring. The first hypothesis relates to the number of consecutive data points, n, required to give a positive detection result. Figure 14 shows where the positive detection would occur when n is 5, 10, and 20. The first two lines, when n is 5 and 10, appear to occur relatively close to where the data begins to diverge. The risk with a low n value is that false positives are more likely to occur. As n was lowered, false positives became more frequent as expected. When a false positive did not occur, the paper cup was still crushed, suggesting that there is a different issue at play.

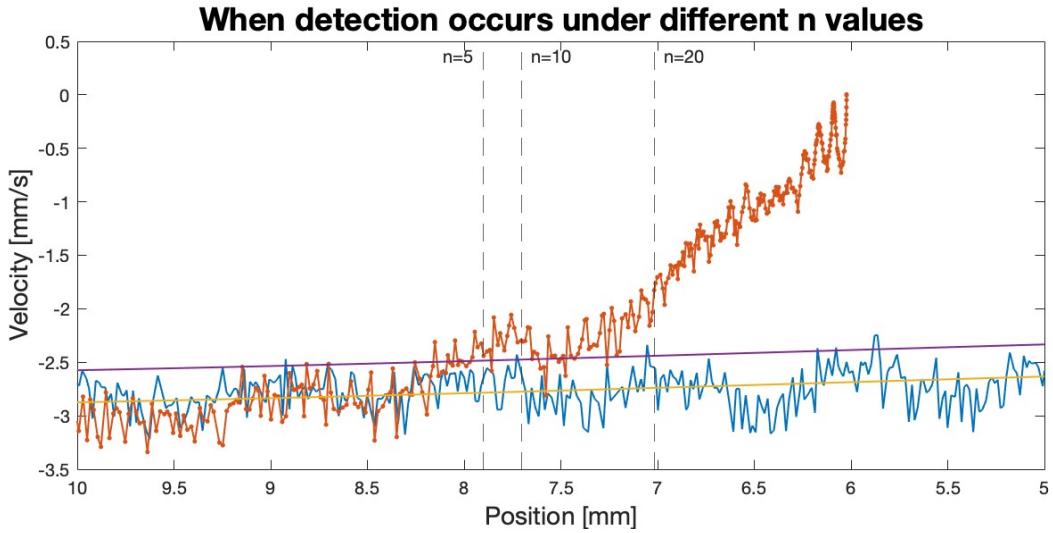

Figure 14. Difference in detection time with varying values of n. The value n is the number of consecutive data points that must fall above the expected velocity threshold (purple) to be considered a detection. A larger value of n causes a longer lag between the actual time of contact and detection.

After tuning the n value did not work, another hypothesis was explored. Until now, it was assumed that the contact was made with the cup close to where a visible divergence in velocity values from the baseline occurred. The results from the above tests suggest that perhaps contact was made much earlier and the divergence occurs after damage has already been caused. To test this hypothesis, the cup data was recollected, but this time with two event markers, the first when contact first occurs and the second when damage to the cup begins. These events can be observed in Figure 15.

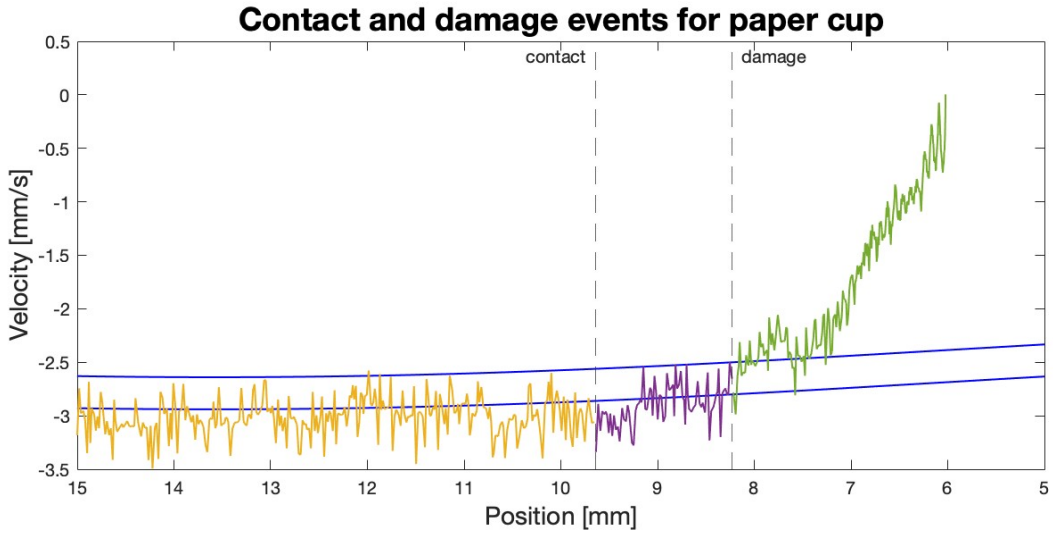

Figure 15. Event markers showing when contact is made with the paper cup versus when damage occurs. Both events happen before detection was determined by the existing algorithm.

The results of this experiment confirm the second hypothesis. By the time there is enough velocity data points above the threshold to determine that an object is present, the cup has already experienced permanent damage. Given that there is no measurable difference between the baseline data and the data from the cup trial between the point of contact and when damage starts to occur other avenues for detection must be explored.

4.5. Adjusted approach

In the previous section, it was discovered that damage was occurring to the paper cup before the algorithm would be able to confirm detection. The window of time between contact and damage to the object was simply too short. In other words, for this highly compliant object, the gripper was moving too fast. The input current of -150 mA was originally chosen because it was the lowest current that could set the jaws in motion; however, once the jaws are moving, they can continue moving under a lower input current. The process described in sections 4.2 and 4.3 were repeated but this time, using an input current of -150 mA to begin closing the gripper and then stepping down to -75 mA. The graph in Figure 16 shows the velocity measurements with respect to position, again with multiple runs to confirm repeatability.

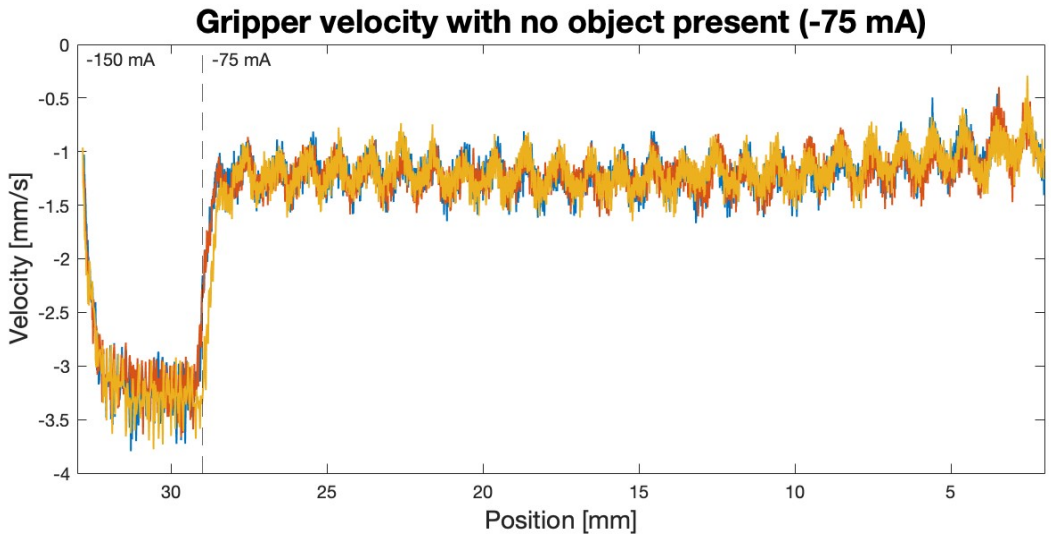

Figure 16. Gripper velocity with respect to position when no object is present when using an input current of -75 mA. The current is set to -150 mA initially to ensure that the gripper is set in motion.

The same process described in Section 4.3 was repeated with the velocity data resulting from the input current of -75 mA. The regression model and its offset are shown overlaid on the velocity data in Figure 17.

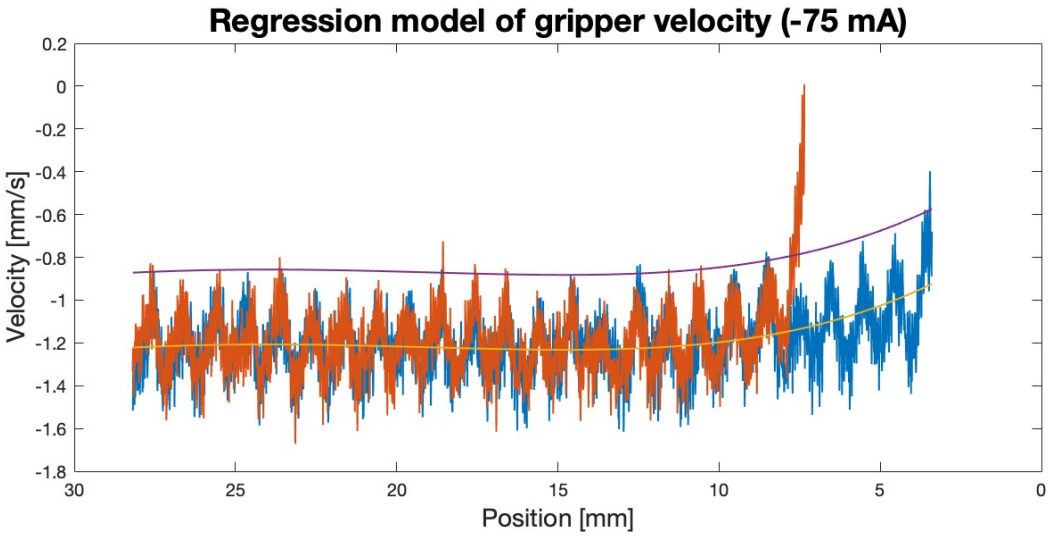

Figure 17. Regression model of expected gripper velocity with respect to position when using an input current of -75 mA. The blue data set is the velocity when no object is present, while the red data is the velocity when a paper cup is present. A regression line (yellow) based on the blue data models the expected velocity of the gripper at each position. This line was offset (purple) to act as a threshold for detection.

Using the same process outlined in Figure 13 in Section 4.3, the detection algorithm was tested again on the paper cup, this time using the input current of -75 mA. The paper cup was successfully without causing permanent damage 30 times out of 30 trials. To ensure that this algorithm would also work on fragile objects, it was tested on potato chips and also succeeded five times out of five trials. Figure 18 shows both the paper cup and the potato chip after detection.

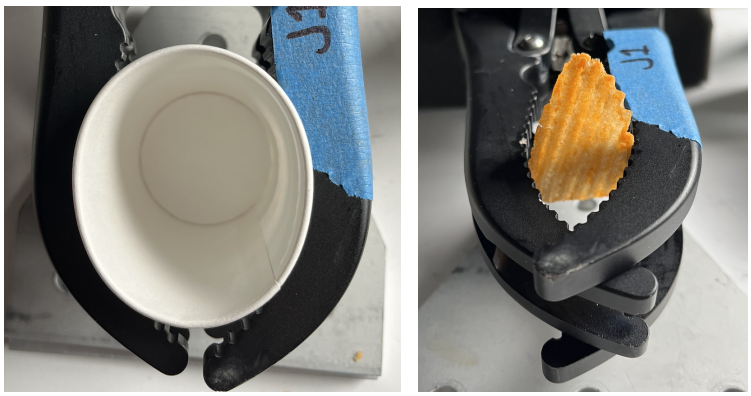

Figure 18. A paper cup (left) and potato chip (right) picture without damage after detection.

5. Characterization

The goal for this portion of the project was to characterize an unknown object in terms of rigidity and strength. Objects were to be placed into one of four categories: rigid and strong, rigid and fragile, compliant and strong, or compliant and fragile. Figure 19 provides a visual representation of how objects will be characterized, as well as four objects used for baseline data collection. The x-axis represents the rigidity of an object, spanning from compliant to rigid, while the y-axis represents the strength of an object, spanning from fragile to strong. Where an object falls within the grid is determined relative to the four base objects, each representing an extreme case of each quadrant.

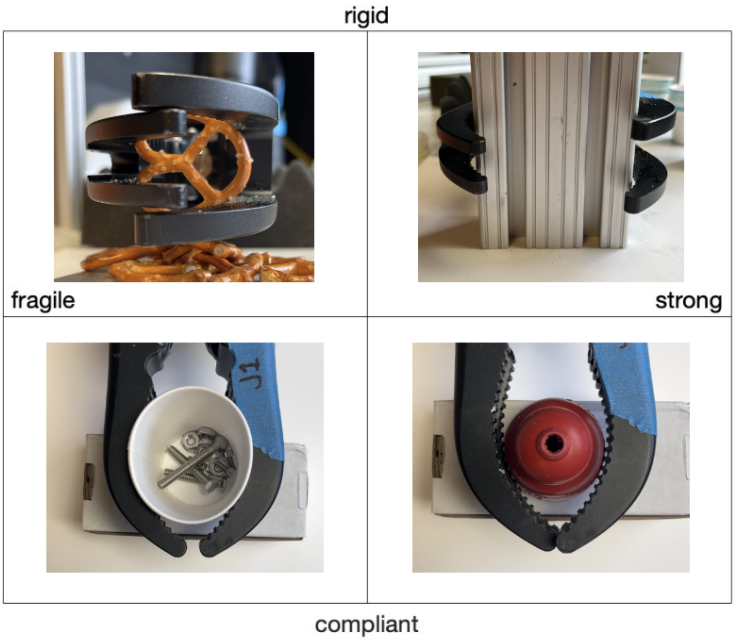

Figure 19. Characterization grid for objects in terms of strength and rigidity. Four objects representing each region are pictured: pretzel (upper left), metal (upper right), paper cup (lower left) and rubber dog toy (lower right). These objects are used in the development of the characterization algorithm discussed in this section.

With the desired characteristics and extreme cases established, a quantitative method to determine these characteristics was needed. An initial experiment was conducted on the four baseline objects in hopes of producing data that showed patterns related to both strength and rigidity. For this experiment, each object was positioned inside the jaws with the jaws set either touching or in very close proximity to the object, as shown in Figure 19. The actuator current was then set to -150 mA for 400 samples, increased to -250 mA for another 400 samples, and then reduced to 0 mA for a final 400 samples. The velocity of the gripper was recorded with each sample and can be seen in Figure 20 below.

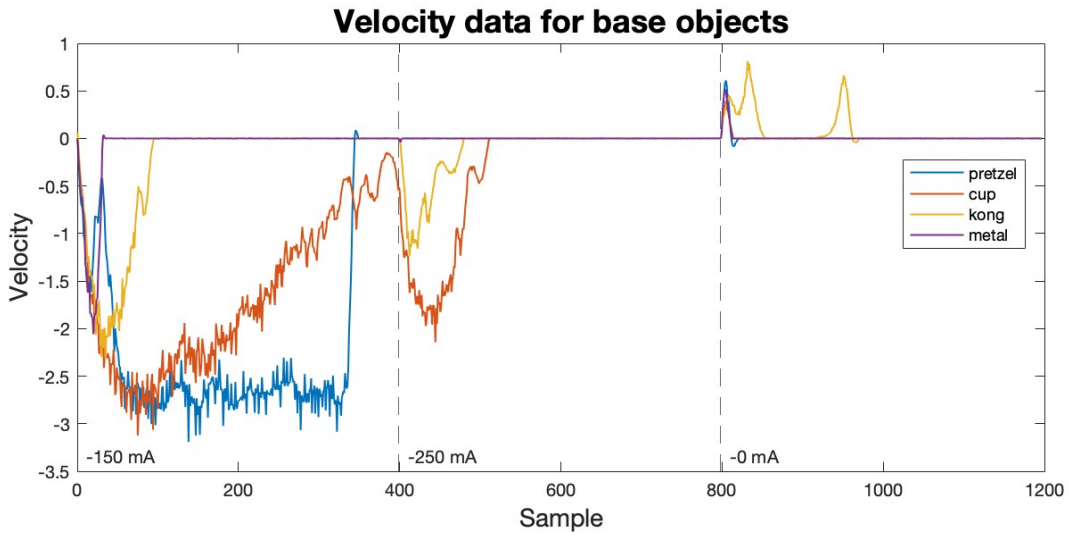

Figure 20. Velocity data under -150 mA, -250 mA, and 0 mA for four different objects for characterization. The data collected in this experiment will be used to develop a method for characterizing objects.

The first third of the graph where the current is held at -150 mA shows insightful information already. Figure 21 shows a closer view of this section. First analyzing the rigid metal piece, the gripper initially accelerates and then decelerates at a quicker rate than in the case of the kong and then paper cup, suggesting that the object is rigid. The kong displays similar behavior, but causes a slower deceleration than the metal piece. For the paper cup, there is a clear decrease in speed, but under -150 mA, the gripper does not stop, suggesting compliant and fragile characteristics. Finally, the data from the pretzel run is the most unique of the four objects. The gripper accelerates initially followed by a momentarily steep deceleration, as would be expected given the rigidity of a pretzel. Before stopping, however, the gripper begins to accelerate again and then maintains a relatively constant velocity for the remainder for the samples. This behavior is explained by the fact that the pretzel broke and was dropped early on in the experiment, leading to the expected conclusion that while the object is rigid, it is also fragile.

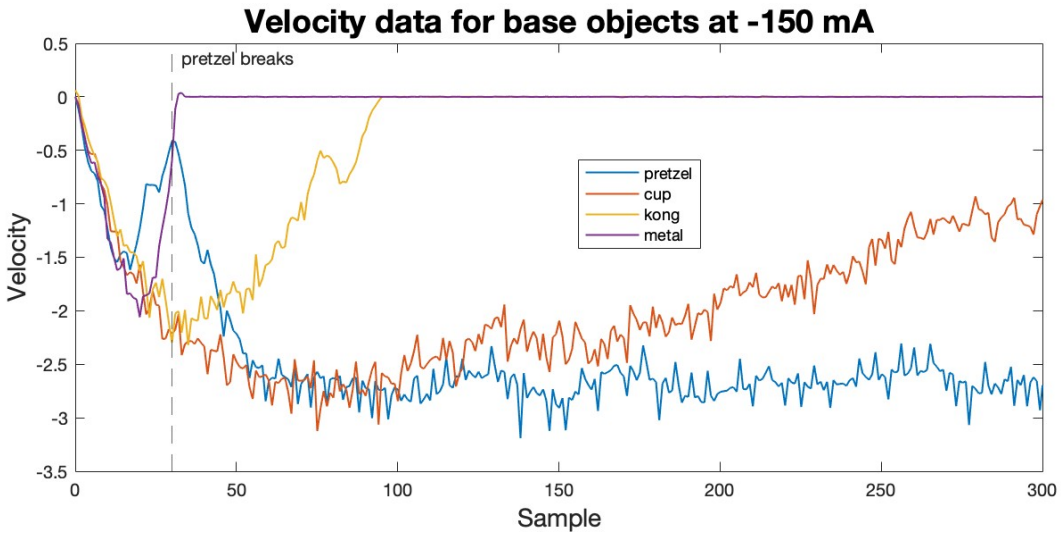

Figure 21. Velocity data under -150 mA, for four different objects. This visual is used to infer properties of each object. dashed vertical line shows the fracture point of the pretzel.

After analyzing the data from the first third of the experiment, when the current was held at -150 mA, it seemed that significant conclusions could be reached about the strength and rigidity of each object. The next step was to develop an automated process for analyzing the data, as opposed to a human analyzing the graphs. The challenge was to extract the key features from the data needed to draw conclusions. Based on the analysis described above, the following process was developed:

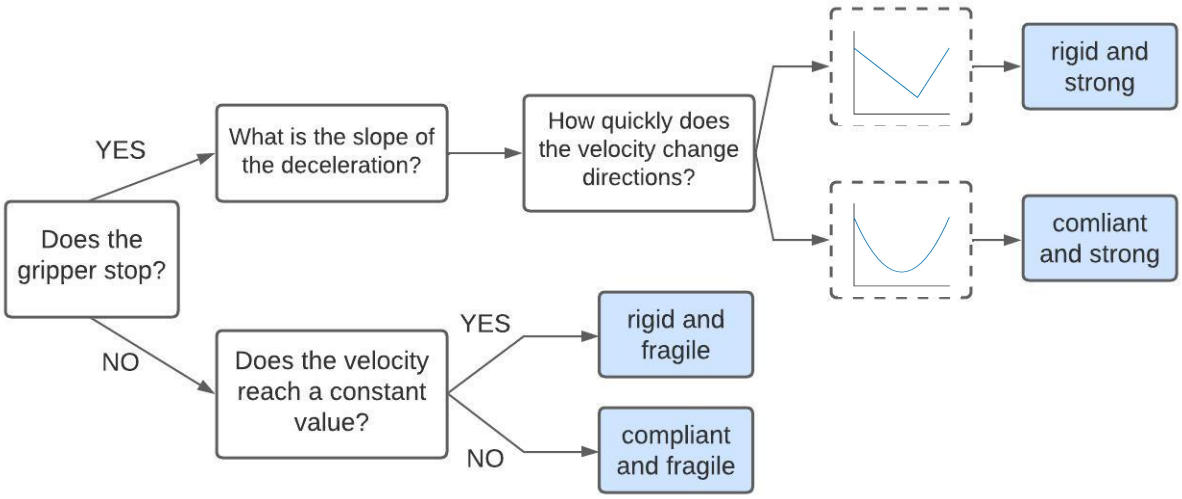

Figure 22. The process for used characterizing an object. If the gripper stops within a set time frame, the deceleration is analyzed to distinguish between a rigid and strong object and a compliant and strong object. If the gripper does not stop and the velocity maintains a relatively constant value, it is assumed that a rigid and fragile object was present but then broke. Otherwise, the object is categorized as compliant and fragile.

Using the process shown in Figure 22, rigid-fragile objects and compliant-fragile objects were easily identified. The first part of the characterization process checks whether the gripper stops moving sometime after making contact with the object. If it does not, the next step is to determine if the velocity was approaching zero or if it maintained a constant velocity expected when no object is present. If the data showed deceleration, the object was characterized as fragile and compliant. If there was no deceleration, the object was characterized as fragile and rigid which is consistent with the idea that the object was broken and dropped. The table in Figure 23 shows the objects tested and how they were characterized based on the process just described. The most fragile objects, the pretzel, foam block, and paper cup, were characterized in the same class each time.

	metal	nalgene	eraser	box	kong	orange	cup	pretzel
Rigid fragile								4
Rigid strong	4	4	2	2				
Compliant fragile							4	
Compliant strong			2	2	4	4		
total	4	4	4	4	4	4	4	4

Figure 23. The results from the characterization process. Each object was tested four times. The number in each box shows how many times each object was characterized with the respective characteristics.

For stronger objects, differentiating between rigid and compliant properties was more challenging using only the data from when -150 mA was being applied to the object. The initial method used to do so involved looking at the rate of deceleration after contact with the object was made. Cutoff values for the time to reach zero velocity after contact were determined from preliminary data of both the kong and the metal piece.

6. Final Results and Discussion

With the ability to detect objects, the alternating position/current command method described in Section 3.2 was no longer necessary. Instead, the detection method could be used to close the grippers until contact with an object was made, at which point an

appropriate current could be set based on known object properties or those determined from the characterization process. Figure 24 shows the successful grasps of a variety of objects, including fragile and brittle objects as well as fragile and compliant objects. Each row of pictures shows objects with relatively similar properties. The first row (a-c) shows three very light, brittle objects. The second row (d-f) of objects are heavier and stronger than the first, but are also prone to fracturing. In the third row (g-i), three highly compliant objects are shown. These objects were the most challenging to detect and motivated the development of the detection portion of this research. The fourth row (j-l) of objects show objects that have compliance but also risk fracturing. And finally, the last row (m-o) shows fruits and vegetables that are heavier and stronger than many of the other test objects, but have sensitive surfaces.

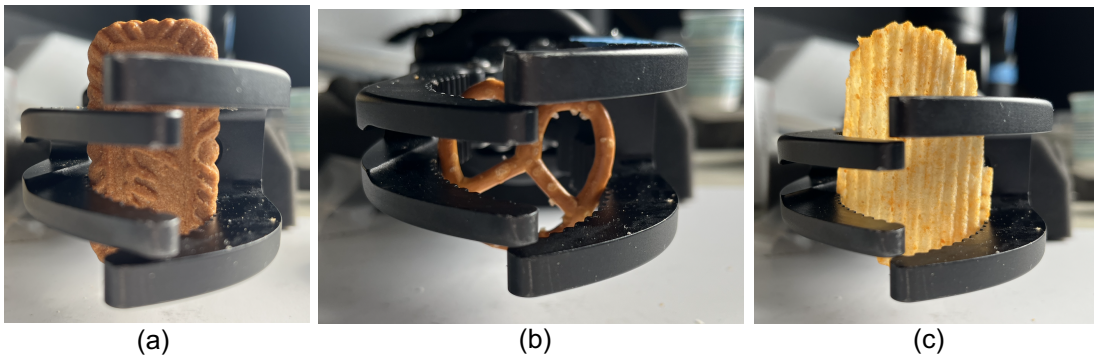

(a) (b) (c)

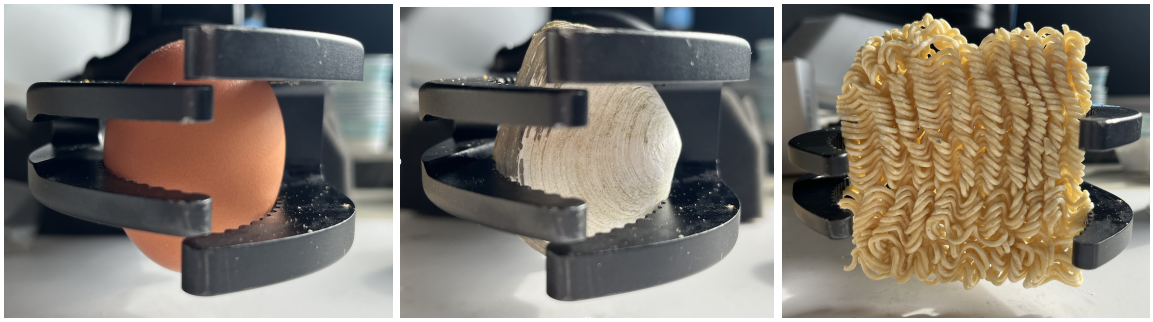

(d) (e) (f)

(g) (h) (i)

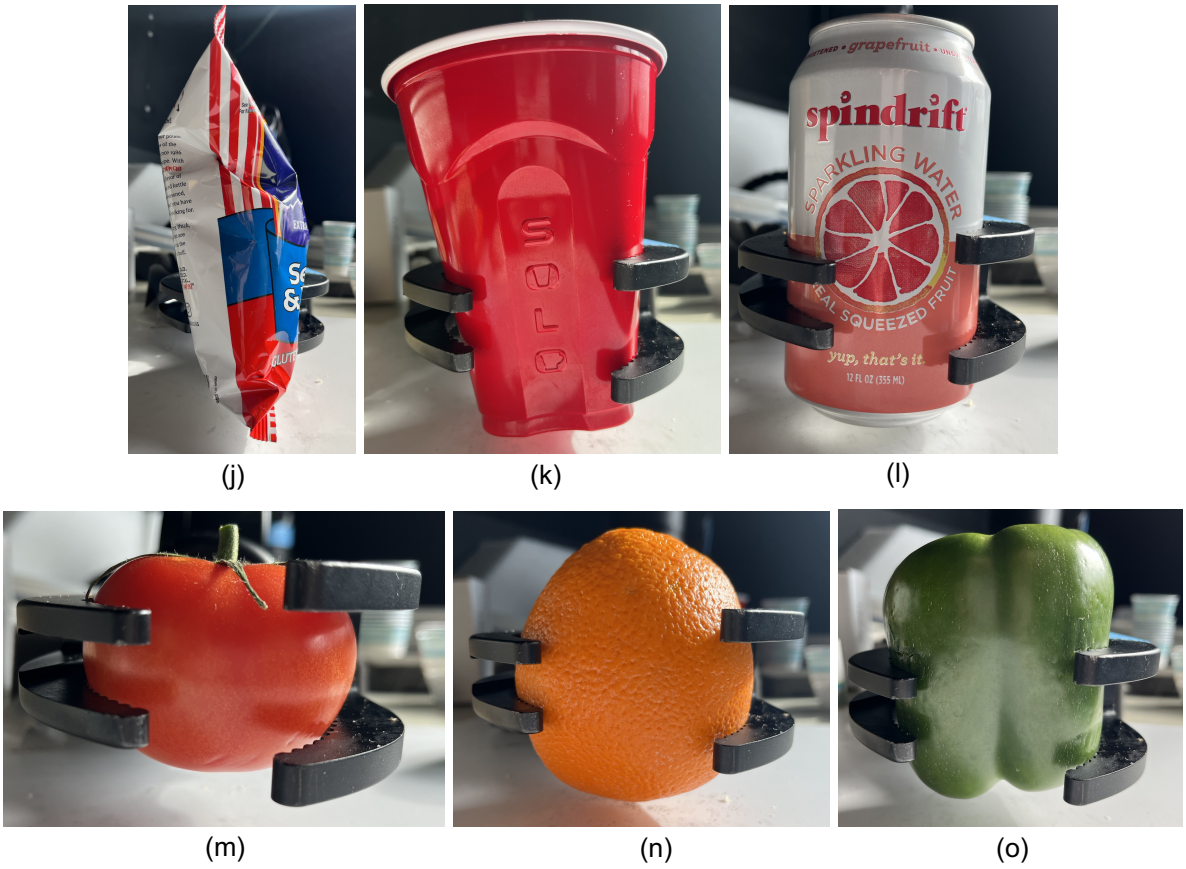

(j) (k) (l)

(m) (n) (o)

Figure 24. Final grasp results. These pictures highlight the range of objects that can be successfully grasped by the rigid gripper used in this research. The objects shown include a biscuit, a pretzel, a potato chip, an egg, a shell, dry ramen noodles, a piece of foam, a paper cup, a bun, a bag of chips, a plastic cup, an aluminum can, a tomato, an orange, and a bell pepper.

All objects were held securely with low input currents between -100 mA and +50 mA. While the rigidity of the gripper was generally a disadvantage when applying gentle grasps, it was helpful when grasping heavier objects as it allowed for a lower applied force. Despite the variation in test object properties, the grasping algorithm enabled a rigid gripper to apply a successful grasp to each object.

7. Conclusion

The goal of this research was to use an off-the-shelf rigid gripper to automatically grasp objects of different strengths and compliances without any additional hardware and without causing damage. Once it was determined that a gentle grasp was possible, a process for detecting and, in some cases, characterization was needed to slowly contact the object before applying an appropriate grasp. This goal was achieved and demonstrated on a variety of objects. This work expands the uses for rigid grippers without sacrificing the high grasp force, robustness, and affordability that is not often found in soft-grippers and other grasping solutions.

The process for grasping in this research only used one orientation, leaving room for even gentler grasps if combined with methods that focus on how to best approach and carry an object. For example, the green bell pepper shown in Figure 24o had slippery vertical sides, requiring more force to securely hold it than the heavier orange in Figure 24n. The shape of the orange enabled it to stay in place with a very light grip. Rotating the bell pepper so that the jaws contacted its top and bottom instead would require less force for a secure grasp. In addition to the grasp approach, rotating the end-effector 90 degrees while holding a delicate object would reduce the risk of slip and allow the robot to loosen its grip.

By combining this research with grasping approach and manipulation algorithms, the versatility of a rigid gripper could be expanded even further. While soft-robotics is making significant strides in developing universal grippers, this research offers a cost-effective solution that can be implemented into existing technology today.

8. Acknowledgements

First and foremost I would like to thank my two advisors, Professor Howard Chizeck and Dr. Aaron Marburg, for providing me with such a unique and invaluable opportunity to be a part of this research. It has allowed me to develop skills and confidence that I never imagined I could have when I first started this program. I would also like to thank Professor Kim Ingraham for her mentorship both as an instructor and a researcher. Her ability to foster engagement and critical thinking has had a profound influence on how I approach engineering problems. Finally, I would like to thank the Office of Naval Research for providing the funding for this project.

9. References

[1] Daniel Cardin-Catalan, Simon Ceppetelli, Angel P. del Pobil, Antonio Morales, Design and analysis of a variable-stiffness robotic gripper, Alexandria Engineering Journal, Volume 61, Issue 2, 2022, Pages 1235-1248, ISSN 1110-0168, https://doi.org/10.1016/j.aej.2021.06.045.

[2] Zhang Long *et al* 2020 *IOP Conf. Ser.: Mater. Sci. Eng.* 782 042055.

[3] Ashutosh Kumar et al 2020 IOP Conf. Ser.: Mater. Sci. Eng. 912 032049.

[4] Terrile S, Argüelles M, Barrientos A. Comparison of Different Technologies for Soft Robotics Grippers. *Sensors*. 2021; 21(9):3253. https://doi.org/10.3390/s21093253.

[5] Hughes J, Culha U, Giardina F, Guenther F, Rosendo A and Iida F (2016) Soft Manipulators and Grippers: A Review. *Front. Robot. AI* 3:69. doi: 10.3389/frobt.2016.00069

[6] A. T. Mathew, I. Hussain, C. Stefanini, I. M. Ben Hmida and F. Renda, "ReSoft Gripper: A reconfigurable soft gripper with monolithic fingers and differential mechanism for versatile and delicate grasping," *2021 IEEE 4th International Conference on Soft Robotics (RoboSoft)*, New Haven, CT, USA, 2021, pp. 372-378, doi: 10.1109/RoboSoft51838.2021.9479341.

[7] S. Li *et al*., "A Vacuum-driven Origami “Magic-ball” Soft Gripper," *2019 International Conference on Robotics and Automation (ICRA)*, Montreal, QC, Canada, 2019, pp. 7401-7408, doi: 10.1109/ICRA.2019.8794068.

[8] R. Maruyama, T. Watanabe and M. Uchida, "Delicate grasping by robotic gripper with incompressible fluid-based deformable fingertips," *2013 IEEE/RSJ International Conference on Intelligent Robots and Systems*, Tokyo, Japan, 2013, pp. 5469-5474, doi: 10.1109/IROS.2013.6697148.

[9] L. Gerez, C. -M. Chang and M. Liarokapis, "A Hybrid, Encompassing, Three-Fingered Robotic Gripper Combining Pneumatic Telescopic Mechanisms and Rigid Claws," *2020 IEEE International Symposium on Safety, Security, and Rescue Robotics (SSRR)*, Abu Dhabi, United Arab Emirates, 2020, pp. 142-147, doi: 10.1109/SSRR50563.2020.9292622.

[10] J. -S. Shaw and V. Dubey, "Design of servo actuated robotic gripper using force control for range of objects," *2016 International Conference on Advanced Robotics and Intelligent Systems (ARIS)*, Taipei, Taiwan, 2016, pp. 1-6, doi: 10.1109/ARIS.2016.7886619.

[11] G. B. Mahanta, A. Rout, B. B. V. L. Deepak, B. B. Biswal and B. M. Gunji, "Preliminary Design and Fabrication of Bio-Inspired Low-Cost Hybrid Soft-Rigid Robotic Hand for Grasping Delicate Objects," *2019 9th Annual Information Technology, Electromechanical Engineering and Microelectronics Conference (IEMECON)*, Jaipur, India, 2019, pp. 17-23, doi: 10.1109/IEMECONX.2019.8876981.

[12] Tang Z, Lu J, Wang Z, Ma G. The development of a new variable stiffness soft gripper. *International Journal of Advanced Robotic Systems*. September 2019. doi:10.1177/1729881419879824.

BLUEPRINTLAB

REACH BRAVO • RB-7001

BRAVO 7

A Tough, 7-Function Manipulator for Inspection Class Vehicles

All Electric

Be Confident.

The Bravo 7 is a 7-Function manipulator that opens up new compact inspection and intervention opportunities for service providers, researchers, and other operators.

Designed to conduct tasks usually reserved for human divers, the arm's dexterity and responsiveness pave the way for advanced applications.

The form factor was specifically designed for industry leading inspection-class ROVs making it a ready-to-go option for existing fleets.

Designed for Leading ROV's

Master Controller Enabled

FEATURES

- Ready-built and designed for industry leading inspection-class vehicles
- Master Arm Controlled
- All-Electric, Zero Oil
- End effectors: grabbers, probe handlers, cutters (or BYO)
- Advanced software interface with 3D visualisation
- Adjustable grab force - pick up a sea urchin or cut a cable
- One-click deploy/stow position

DEXTEROUS
7-Function (or custom fit)
Highly Modular & Configurable

RUGGED
300m Depth Rating
10kg Full Reach Lift

SMART
In-Built Kinematics
Master Arm Controlled

Mission Specific End-Effectors | Interchange With Ease

Parallel Jaws

SS Wide Quad Jaws

Quad Jaws

Cable Cutter

Interlocking Quad Jaws

BLUEPRINTLAB

SPECIFICATIONS

Reach	0.9m
Full Reach Lift	10kg
Max Lift Capacity	20kg
Joint Speed	60deg/s nominal
End-effector Accuracy	<1cm
Grabber Close Force	1000N
Optional Sensor Interface	PWR + 485 + Ethernet
Control Modes	Position, Velocity, Cartesian (XYZ)

Power Interface	
Bulkhead	MCBH4M – MC 4C Male
Pigtail	MCIL4F – MC Inline, 4C Female, 60cm
Comms Interface	
Bulkhead	MCBH8ME – MC Ethernet, 8C Male
Pigtail	MC Ethernet Inline, 8C Female 100cm

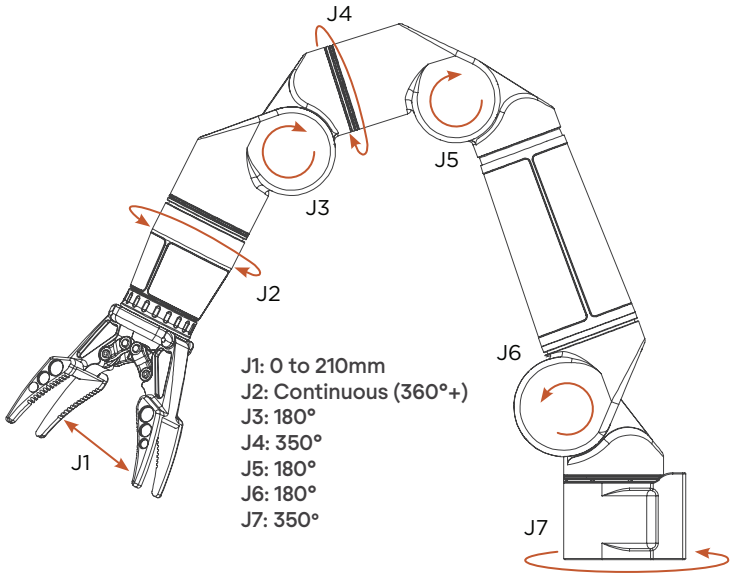

J1: 0 to 210mm
J2: Continuous (360°+)
J3: 180°
J4: 350°
J5: 180°
J6: 180°
J7: 350°

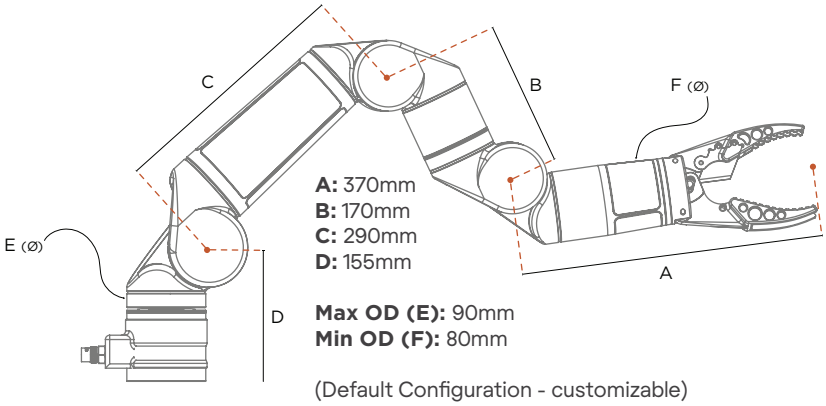

A: 370mm
B: 170mm
C: 290mm
D: 155mm

Max OD (E): 90mm
Min OD (F): 80mm

(Default Configuration - customizable)

ELECTRICAL

Voltage	20-48V
Nominal Power	200W (10kg Load)
Peak Power	300W (10kg Load)
COMS	RS232/RS485/Ethernet

ENVIRONMENTAL

Depth	300MSW
Temp	-10°C to 35°C
Material	AL6061

MECHANICAL

Lift Capacity	10kg (full reach)
Max Lift	20kg
Weight (Air)	9.5kg
Weight (Water)	4.5kg

High Mobility & Compact

Note: base joint is software limited to 350° (not continuous)

TOP VIEW

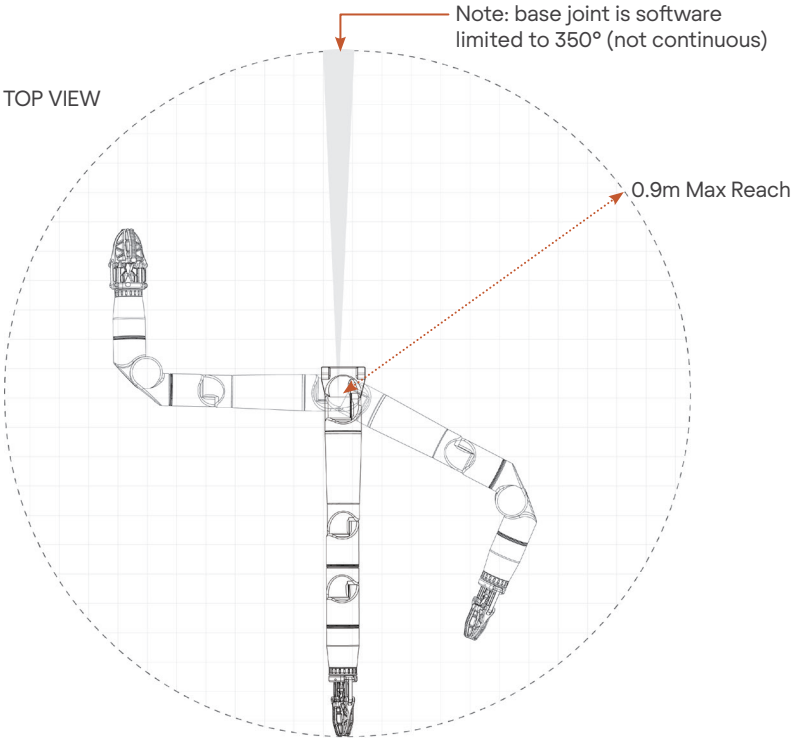

SIDE VIEW